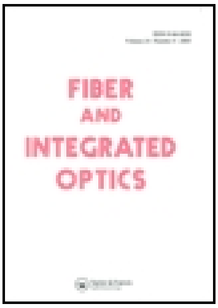

Fiber and Integrated Optics
Publication details, including instructions for authors and subscription information:
http://www.tandfonline.com/loi/ufio20

Phase perturbation investigation of laser diode for the laser diode to single-mode fiber coupling system

Haiming Wang [a b]

[a] National Applied Optics Laboratory (NAOL), Changchun Institute of Optics and Fine Mechanics (CIOFM), Chinese Science Academy, Changchun, China

[b] Lehrstuhl für Feinwerktechnik, Universität kaiserslautern, Erwin-Schödinger-Straße, 6750, Kaiserslautern, Germany

Published online: 20 Aug 2006.

To cite this article: Haiming Wang (1991): Phase perturbation investigation of laser diode for the laser diode to single-mode fiber coupling system, Fiber and Integrated Optics, 10:3, 245-256

To link to this article: http://dx.doi.org/10.1080/01468039108219338

Fiber and Integrated Optics, Volume 10, pp. 245–256
0146-8030/91 $3.00 + .00

Phase Perturbation Investigation of Laser Diode for the Laser Diode to Single-mode Fiber Coupling System

HAIMING WANG

National Applied Optics Laboratory (NAOL)
Changchun Institute of Optics and Fine Mechanics (CIOFM)
Chinese Science Academy
Changchun, China

Abstract *A novel phase-perturbation method as well as an experimental system were established to study the deviation of the laser diode (LD) far-field intensity distribution from the ideal Gaussian. An analytical expression of the LD far-field intensity distribution and a numerical method based on the Monte Carlo calculation were developed to fit the measured results. The loss of the LD to the single-mode fiber (SMF) coupling system caused by this kind of deviation of the LD far-field intensity distribution was quantitatively analyzed.*

Introduction

Coupling light from laser diode (LD) to single-mode fiber (SMF) is a rather important task for the optical communication system. Generally the power-coupling efficiency c is determined by the Fresnel loss, which is expressed by a factor R_f, and the overlap between the normalized LD far-field U_2 and the normalized SMF far-field U_F (propagating through the coupling optics) [1]:

$$c = R_f \left| \iint_{-\infty}^{\infty} U_2(x, y) U_F^*(x, y) \, dx \, dy \right|^2 \tag{1}$$

It is well understood that the propagation mode of the SMF is nearly perfect Gaussian, while the near field of the LD can be approximately expressed by an elliptical Gaussian function with different spot sizes in the direction parallel and perpendicular to the LD junction, respectively. Many papers have discussed the losses caused by the ellipticity of the LD near field and the spot mismatch between the far field of the LD and the SMF [2, 3], as well as by the aberrations of the coupling optics [4]. The Fresnel loss caused by the reflection at the surfaces of the coupling optics can always be reduced by the antireflection (AR) coatings, while the scattering loss caused by the roughness of those surfaces can also be briefly expressed by the total integrated scattering (TIS) [5].

However, a significant factor inducing loss remains for thorough discussion. The

Haiming Wang's present address is: Lehrstuhl für Feinwerktechnik, Universität Kaiserslautern, Erwin-Schödinger-Straße 6750 Kaiserslautern, Germany.
Received: December 4, 1991; accepted: December 18, 1991.

elliptical Gaussian is far from an exact expression of the LD near field. Experiments have shown that the LD far-field intensity distribution deviates from the Gaussian mode, even with some fine structures [6]. This deviation naturally reduces its overlap with the SMF far field and causes loss, experimentally estimated in the range of 0.1 to 1 dB, with the typical value about 0.5 dB [7–13]. This phenomenon obviously indicates that there must be a phase perturbation in the near field, which could be induced by some random process such as the roughness of the LD exit-mirror surface and its waveguide interfaces or by the inhomogeneity of the waveguide materials. These processes would make the near-field light scattered and finally induce the far-field intensity deviated from the elliptical Gaussian mode.

Now we confront a special difficulty: Since we could measure only the far-field intensity distribution, if we want to determine the coupling efficiency directly using Eq. (1), we should retrieve the phase information from the measured intensity distribution, which is an extremely difficult process, particularly when the random property of the near field should be taken into consideration. In this paper, we have achieved an important result, namely, that we could apply the intensity instead of the complex amplitude of the LD far field to determine the coupling efficiency, making the complicated phase-retrieval process no longer necessary.

Theoretical Background

Considering an LD with wavelength λ, the emitted laser beam in the near-field plane (exit mirror surface) can be generally expressed by a wave function

$$U_1(\xi, \eta) = A(\xi, \eta) \exp [i\varphi(\xi, \eta)] \tag{2}$$

with amplitude A, phase φ, and near-field coordinates ξ and η (parallel and perpendicular to the LD junction, respectively). With the definition of the Fourier transform

$$\mathrm{FT}[f(\xi, \eta)] = \int_{-\infty}^{\infty}\!\!\int f(\xi, \eta) \exp [-i2\pi(u\xi + v\eta)]\, d\xi\, d\eta \tag{3}$$

we can express the far-field distribution [14]

$$U_2(x, y) = \frac{1}{\lambda R} \mathrm{FT}[U_1(\xi, \eta)] \tag{4}$$

with the spatial frequencies u and v, which are defined by the far-field coordinates x and y (parallel and perpendicular to the LD junction, respectively), as well as the far-field polar angle ϑ and azimuthal angle φ, the wave vector $\mathbf{k} = (k_x, k_y, k_z)$, and the distance R between the near-field and the far-field planes, respectively,

$$u = \frac{k_x}{2\pi} = \frac{x}{\lambda R} = \frac{\sin\vartheta\cos\varphi}{\lambda}$$
$$v = \frac{k_y}{2\pi} = \frac{y}{\lambda R} = \frac{\sin\vartheta\sin\varphi}{\lambda} \tag{5}$$

as shown in Fig. 1.

Considering that the near-field phase is induced by some random process, we should average Eq. (1) by a stochastic process to determine the coupling efficiency c:

$$c = R_f\left\langle\left|\iint_{-\infty}^{\infty} U_2(x, y)U_F^*(x, y)\,dx\,dy\right|^2\right\rangle$$
$$= R_f\iint_{-\infty}^{\infty}\iint_{-\infty}^{\infty}\langle U_2(x, y)U_2^*(x', y')\rangle U_F^*(x, y)U_F(x', y')\,dx\,dy\,dx'\,dy' \tag{6}$$

Now let us consider the mutual intensity

$$J(x, y; x', y') = \langle U_2(x, y)U_2^*(x', y')\rangle$$
$$= \left\langle\iint_{-\infty}^{\infty}\iint_{-\infty}^{\infty} U_1(\xi, \eta)U_1^*(\xi', \eta')\exp\{-i2\pi[(u\xi - u'\xi') + (v\eta - v'\eta')]\}\,d\xi\,d\eta\,d\xi'\,d\eta'\right\rangle\Big/(\lambda R)^2$$
$$= \frac{1}{(\lambda R)^2}\iint_{-\infty}^{\infty}\iint_{-\infty}^{\infty}\langle U_1(\xi, \eta)U_1(\xi', \eta')\rangle\exp\{-i2\pi[(u\xi - u'\xi') + (v\eta - v'\eta')]\}\,d\xi\,d\eta\,d\xi'\,d\eta' \tag{7}$$

Let

$$\xi - \xi' = p$$
$$\eta - \eta' = q \tag{8}$$

substituting Eq. (2) to Eq. (7), and applying the elliptical Gaussian function with spot sizes ω_x and ω_y (parallel and perpendicular to the LD junction, respectively),

$$A(\xi, \eta) = \frac{2}{\pi\omega_x\omega_y}\exp\left[-\left(\frac{\xi^2}{\omega_x^2} + \frac{\eta^2}{\omega_y^2}\right)\right] \tag{9}$$

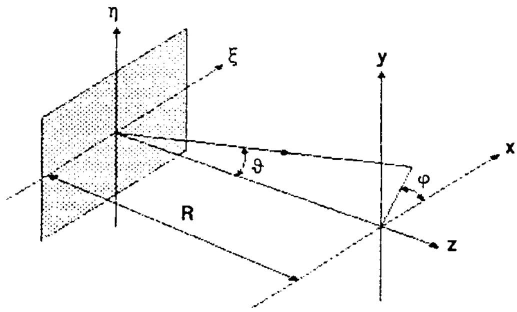

Figure 1. The LD near-field and far-field planes versus the spatial frequencies.

which yields the mutual intensity

$$J(x, y; x', y') = \int\int_{-\infty}^{\infty} \int\int_{-\infty}^{\infty} A(\xi, \eta) A(\xi - p, \eta - q) S(p, q) \exp \{ -i2\pi[\xi(u - u') + \eta(v - v')]\} \exp[-i2\pi(u'p + v'q)]\, d\xi\, d\eta\, dp\, dq \Big/ (\lambda R)^2$$
$$= \frac{1}{(\lambda R)^2} \exp \{ -\pi^2[\omega_x^2(u - u')^2 + \omega_y^2(v - v')^2]\} \times \int\int_{-\infty}^{\infty} G(p, q) S(p, q) \exp \left\{ -i2\pi \left[\frac{p}{2}(u + u') + \frac{q}{2}(v + v') \right] \right\} dp\, dq \tag{10}$$

with

$$G(p, q) = \exp \left[-\frac{1}{2} \left(\frac{p^2}{\omega_x^2} + \frac{q^2}{\omega_y^2} \right) \right] \tag{11}$$

representing the transfer of near-field amplitude to the far field, and

$$S(p, q) = \langle \exp \{ i[\varphi(\xi, \eta) - \varphi(\xi - p, \eta - q)]\} \rangle \tag{12}$$

representing the influence of the near-field phase on the far-field intensity distribution. When the probability law describing the random process of the near-field phase is given, integration of Eq. (12) yields a definite $S(p, q)$ function.

On the other hand, by a similar average process, we could obtain the far-field intensity distribution

$$I_2(x, y) = \langle U_2(x, y)U_2^*(x, y)\rangle$$
$$= \frac{1}{(\lambda R)^2}\int\int_{-\infty}^{\infty} G(p, q)S(p, q)\exp[-i2\pi(up + vq)]\, dp\, dq \qquad (13)$$

Comparing Eq. (10) with Eq. (13), we can express the mutual intensity by the intensity distribution instead of the complex amplitude of the LD far field

$$J(x, y; x', y') = 4\exp\{-\pi^2[\omega_x^2(u - u')^2 + \omega_y^2(v - v')^2]\} \times I_2\left(\frac{x + x'}{2}, \frac{y + y'}{2}\right) \qquad (14)$$

Loss Analysis

Equation (14) proves that the coupling efficiency could be simply determined by the LD far-field intensity distribution. We start to study it by means of the central limit theorem [15], which permits us to assume that the random process describing the near-field phase φ has a Gaussian probability density function with zero mean value and the root-mean-square (rms) value σ:

$$p(\varphi, \varphi') = \frac{1}{2\pi\sqrt{1 - C^2}}\exp\left[-\frac{\varphi^2 + \varphi'^2 + 2C\varphi\varphi'}{2\sigma^2(1 - C^2)}\right] \qquad (15)$$

with the definition of the autocorrelation function

$$C(p, q) = \frac{\langle\varphi(\xi, \eta)\varphi(\xi - p, \eta - q)\rangle}{\sigma^2} \qquad (16)$$

and

$$\varphi' = \varphi(\xi - p, \eta - q) \qquad (17)$$

Applying Eqs. (15) and (16) to Eq. (12), we find an analytical expression of the function $S(p, q)$

$$S(p, q) = \exp\{-\sigma^2[1 - C(p, q)]\} \qquad (18)$$

Expanding $S(p, q)$ by a Taylor series

$$S(p, q) = 1 + \sum_{n=1}^{\infty}(-1)^n\frac{\sigma^{2n}}{n!} + \sum_{n=1}^{\infty}\sum_{m=1}^{n}(-1)^{n+m}\binom{n}{m}\frac{1}{n!}C^m(p, q)\sigma^{2n} \qquad (19)$$

with

$$\binom{n}{m} = \frac{n(n - 1)\cdots(n - m + 1)}{m!} \qquad (20)$$

we can express the far-field intensity distribution by the equation

$$I_2(x, y) = (1 - \alpha)I_{2O}(x, y) + I_{2S}(x, y) \tag{21}$$

in which

$$I_{2O}(x, y) = \mathrm{FT}[G(p, q)] = \frac{2\pi\omega_x\omega_y}{(\lambda R)^2} \exp\left[-2\pi^2(\omega_x^2u^2 + \omega_y^2v^2)\right] \tag{22}$$

represents the ideal elliptical Gaussian intensity distribution of the far field without the near-field phase perturbation,

$$I_{2S}(x, y) = \frac{1}{(\lambda R)^2} \sum_{n=1}^{\infty} \sum_{m=1}^{n} (-1)^{n+m} \binom{n}{m} \frac{\sigma^{2n}}{n!} \iint_{-\infty}^{\infty} C^m(p, q)G(p, q) \times \exp\left[-i2(up + vq)\right] dp\, dq \tag{23}$$

represents the part of the far-field intensity distribution scattered by the near-field phase, and

$$\alpha = -\sum_{n=1}^{\infty}(-1)^n\frac{\sigma^{2n}}{n!} = 1 - \exp(-\sigma^2) = \iint_{-\infty}^{\infty} I_{2S}(x, y)\, dx\, dy \tag{24}$$

Consider the near field of the SMF with spot size ω_F, since the scattered part of the LD far-field intensity distribution I_{2S} will no longer be coupled into the SMF. Substituting Eqs. (21), (22), and (14) into (6) yields the coupling efficiency

$$c = R_f(1 - \alpha)\frac{2\omega_x\omega_F}{\omega_x^2 + \omega_F^2}\,\frac{2\omega_y\omega_F}{\omega_y^2 + \omega_F^2} \tag{25}$$

Obviously, factor α represents the loss induced by the near-field phase perturbation, which causes the far-field intensity distribution to be deviated from the ideal elliptical Gaussian. As far as factor α is known, we can determine the coupling efficiency. In the actual application, the loss caused by the near-field phase perturbation can be defined (in dB) as

$$\text{loss} = -10\log_{10}(1 - \alpha) \tag{26}$$

Since the typical value of the loss caused by the deviation of the LD far-field intensity distribution is 0.5 dB (i.e., $\alpha = 1 - 10^{-0.05} = 0.109$), when we employ the first-order approximation of near-field phase perturbation to calculate, from Eq. (23), the far-field intensity distribution, the cutoff error of the higher-order phase-perturbation terms is

$$\left|\frac{\sigma^4}{2}\iint_{-\infty}^{\infty} C^2(p, q)G(p, q)\exp\left[-i2\pi(up + vq)\right] dp\, dq\right| \leq \frac{\sigma^4}{2} \approx \frac{\alpha^2}{2} = 0.00594$$

with the associated loss of 0.026 dB. Comparing with the first-order loss of 0.5 dB, we can simply ignore the higher-order terms of Eq. (23). In this event it is even unnecessary to assume that the near-field phase has a Gaussian probability density function. Let us start from Eq. (2); for the first-order approximation we should employ all terms in Eq. (1) in the order not higher than σ^2:

$$\exp[i\varphi(\xi,\eta)] = 1 + i\varphi(\xi,\eta) - \frac{\varphi^2(\xi,\eta)}{2} \tag{27}$$

$$U_1(\xi,\eta) = A(\xi,\eta)\left[1 + i\varphi(\xi,\eta) - \frac{\varphi(\xi,\eta)}{2}\right] \tag{28}$$

We define the power spectrum function in the area S where the near-field intensity distribution is definitely nonzero:

$$\mathrm{PSD}[f(\xi,\eta)] = \frac{\langle|\mathrm{FT}[f(\xi,\eta)]|^2\rangle}{S} \tag{29}$$

Considering that $\langle\varphi\rangle = 0$, $\langle\varphi^2\rangle = \sigma^2$, we can express the far-field intensity distribution in the form

$$\begin{aligned} I_2(x,y) &= \frac{\langle|\mathrm{FT}[U_1(\xi,\eta)]|^2\rangle}{(\lambda R)^2} \\ &= \frac{1}{(\lambda R)^2}\iint_{-\infty}^{\infty}\iint_{-\infty}^{\infty} A(\xi,\eta)A(\xi',\eta')\left\langle\left[1 + i\varphi(\xi,\eta) - \frac{\varphi(\xi,\eta)^2}{2}\right]\right. \\ &\quad \times \left.\left[1 - i\varphi(\xi',\eta') - \frac{\varphi(\xi',\eta')^2}{2}\right]\right\rangle \exp\{-i2\pi[u(\xi-\xi') \\ &\quad + v(\eta-\eta')]\}\, d\xi\, d\eta\, d\xi'\, d\eta' \\ &= \frac{1-\sigma^2}{(\lambda R)^2}\left|\iint_{-\infty}^{\infty} A(\xi,\eta)\exp[-i2\pi(u\xi + v\eta)]\, d\xi\, d\eta\right|^2 \\ &\quad + \frac{1}{(\lambda R)^2}\iint_{-\infty}^{\infty}\iint_{-\infty}^{\infty} A(\xi,\eta)A(\xi',\eta')\langle\varphi(\xi,\eta)\varphi(\xi',\eta')\rangle \\ &\quad \times \exp\{-i2\pi[u(\xi-\xi') + v(\eta-\eta')]\}\, d\xi\, d\eta\, d\xi'\, d\eta' \\ &= (1-\sigma^2)I_{2O}(x,y) + I_{2S}(x,y) \end{aligned} \tag{30}$$

similar to Eq. (22). Moreover, the part of the first-order perturbation of the far-field intensity distribution I_{2S} can be expressed

$$I_{2S}(x,y) = \frac{S}{(\lambda R)^2}\,\mathrm{PSD}[A(\xi,\eta)\varphi(\xi,\eta)] \tag{31}$$

which is identical to Eq. (23) except that here it is no longer necessary to assume the Gaussian probability law of the near-field phase.

In the case where the near-field phase is quite large (e.g., when the loss is about 1 dB and the associated rms value of the phase is $\sigma \approx 0.454$), we should take the perturbation orders higher than the first one and apply Eq. (23) to calculate the scattered part of the far-field intensity distribution.

Numerical Method

The correlation method has been applied to obtain some important properties of the LD. Let I_m be the measured far-field intensity distribution, and define the correlation function:

$$\mathrm{corr} = \frac{2\iint_{-\infty}^{\infty} \sqrt{I_m I_2(x, y)}\, dx\, dy}{\iint_{-\infty}^{\infty} [I_m + I_2(x, y)]\, dx\, dy} \tag{32}$$

Here we use the square root of the intensity instead of the intensity itself, since when we normalize the measured and the calculated power to unit

$$1 = \iint_{-\infty}^{\infty} I_m\, dx\, dy = \iint_{-\infty}^{\infty} I_2(x, y)\, dx\, dy \tag{33}$$

the maximization of the correlation of Eq. (32) will be equivalent to the minimization of the fitting error of the least-square fitting

$$\mathrm{err} = \iint_{-\infty}^{\infty} [\sqrt{I_m} - \sqrt{I_2(x, y)}]^2\, dx\, dy \tag{34}$$

between the measured and the calculated far-field intensity distributions.

At first, we fit the measured far-field intensity distribution by the ideal elliptical Gaussian function $I_{2O}(x, y)$. This procedure yields the spot sizes in the directions parallel and perpendicular to the LD junction, ω_x and ω_y, in the near field, respectively.

Then we consider the contribution of the near-field phase perturbation. We apply the Monte Carlo calculation, which could produce a random data set with any probability density we wanted. As an example, if here we still consider that the near-field phase obeys the Gaussian law, then the associated random data set could be expressed

$$\begin{aligned} \varphi_1 &= \sigma\sqrt{-\ln (y_1)} \cos (2\pi y_2) \\ \varphi_2 &= \sigma\sqrt{-\ln (y_1)} \sin (2\pi y_2) \end{aligned} \tag{35}$$

with y_1 and y_2 representing the uniformly distributed random variances in the range of (0, 1), and the rms value σ, respectively [16].

By means of the power-spectrum estimation technique [17], we can calculate the far-field intensity distribution with Eq. (31) from the near-field phase generated by Eq. (35), to fit the measured far-field intensity distribution. This procedure yields the rms of the near-field phase σ, from which we can directly calculate the loss caused by the deviation of the LD far-field intensity distribution from the ideal elliptical Gaussian.

Experimental Results and Discussions

Figure 2 shows a far-field intensity-distribution measurement system, which detects the far-field intensity I_2 dependent on the far-field angle ϑ. An LD (3) with wavelength 1.3 μm is driven by the LD module (2), which is mounted at the center of a rotation stage driven by a stepping motor (1) with resolution 0.01°; at the end of the rotation arm a germanium photodiode (4), with aperture 1 mm diam and sensitive wavelength range from 0.8 to 1.8 μm, is employed as the detector; an LD operation package (9) with the built-in electronic modulation is applied to make the LD emit AC signals, while the reference frequency is sent to a lock-in amplifier (5) to demodulate the signals, then send them to a digital multimeter (6); on the other hand, the motor is operated by a motor controller (8) to pick up the positions of the photodiode; finally, the photocurrent signals from the multimeter as well as the position signals from the motor controller are sent to a Hewlett-Packard PC HP 9836 (7) for further processing.

A Hitachi LD P 5400/E 2964 was measured. Both the measured far-field intensity distributions and the fits in the directions parallel and perpendicular to its junction are shown in Figs. 3 and 4, respectively. Generally, the near-field phase perturbation scatters the light emitted from the LD; therefore, the measured intensity-distribution curves in the large-scattering angle (high-spatial-frequency) region have some nonzero background. When we fit these curves only with the ideal elliptical Gaussian functions, they could not be easily fit in with the actually measured curves since the Gaussian function vanishes very rapidly in the high frequency. As shown in Fig. 3, when a Gaussian function with spot site ω_x = 0.72 μm was employed to fit the measured far-field intensity distribution of the LD in the direction parallel to its junction, the nonzero high-

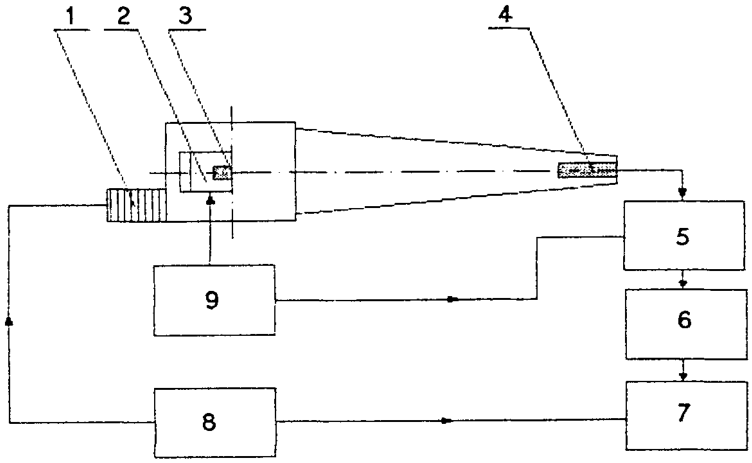

Figure 2. Construction of the experimental system.

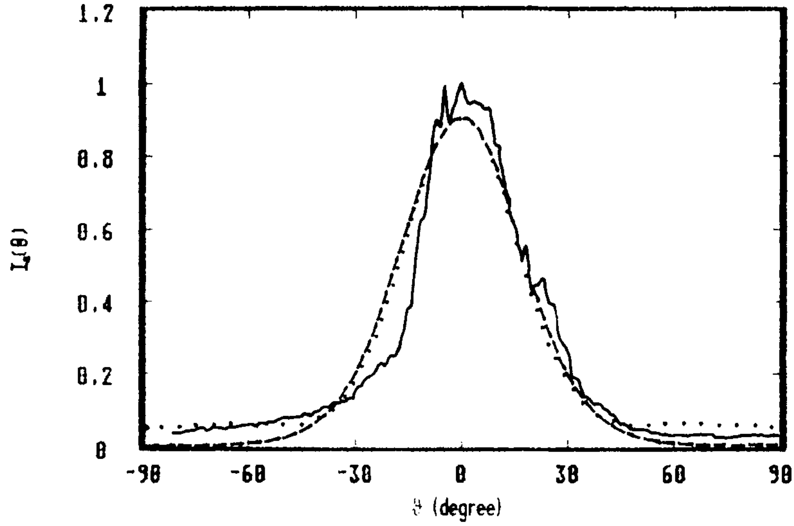

Figure 3. Relative intensity I_2 of LD versus its far-field angle (ϑ, $\varphi = 0$), parallel to its junction. Solid line, measured result; dashed line, fit by ideal Gaussian; dotted line, fit by phase perturbation.

frequency component of the measured result could not be fit by this simple Gaussian function, which yields a correlation of 0.9641. However, if we take the near-field phase perturbation into consideration and use the Monte Carlo calculation, we can generate some high-frequency background to fit the measured result, thereby improving the fitting error. Still shown in Fig. 3, when in this event we generate a calculated far-field intensity distribution with near-field phase perturbation having rms $\sigma^2 = 0.12$ to fit the measured result, the correlation increases to 0.9758.

A similar consequence is expected for the far-field intensity distribution in the direc-

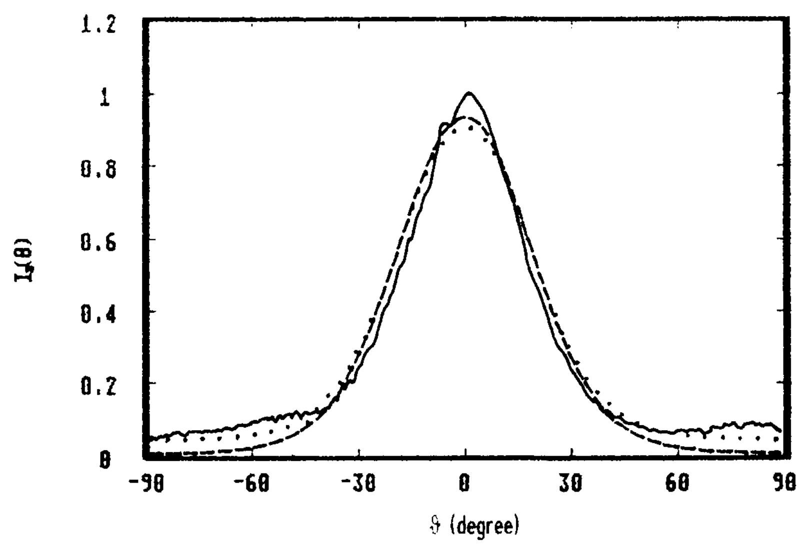

Figure 4. Relative intensity I_2 of LD versus its far-field angle (ϑ, $\varphi = \pi/2$), perpendicular to its junction. Solid line, measured result; dashed line, fit by ideal Gaussian; dotted line, fit by phase perturbation.

tion perpendicular to the LD junction, as shown in Fig. 4. Now the ideal Gaussian function fit gives out the spot size $\omega_y = 0.65$ μm in the near field, with corr = 0.9760; while the Monte Carlo fit gives out the near-field phase with $\sigma^2 = 0.085$, and corr = 0.9867.

From these results, we could deduct the following: at first, the fits, consisting of the influence of the near-field phase, considerably improve the fitting errors; next, the near-field phase also gives out an evaluation of the LD quality. Considering light scattered from the optical surface with rms roughness σ_r, for the normal incidence, we could express the total integrated scattering (TIS) [5] as

$$\text{TIS} = \left(\frac{4\pi}{\lambda}\sigma_r\right)^2 \tag{36}$$

In our applications here, the factor σ^2 plays a role similar to that of the TIS. If we consider the near-field phase as a quite rough "plane," the equivalent roughness of the plane with rms σ_r should be

$$\sigma_r = \frac{\sigma}{4\pi}\lambda \tag{37}$$

For the parallel direction, $\sigma_r \approx \lambda/36$, while for the perpendicular direction, $\sigma_r \approx \lambda/43$.

The associated loss caused by the near-field phase perturbation is about 0.56 dB for the parallel direction and about 0.39 dB for the perpendicular direction.

Conclusions

Generally, the complex amplitude of the LD far field is needed to determine the coupling efficiency of the LD-to-SMF system. The difficulty is that only the intensity distribution of the LD far field could be measured. In this paper, a novel method was developed to solve this problem: The coupling efficiency was expressed by the intensity distribution instead of the complex amplitude of the LD far field, thus avoiding the extremely complicated phase-retrieval process.

Next, an analytical expression of the far-field intensity distribution, including distribution of the near-field phase by employment of the Monte Carlo calculation, was deduced. This expression could be used to fit the actually measured far-field intensity distribution. The results reported in this paper show that such a fit is valid and applicable.

Moreover, this deduced analytical expression could be applied to some situations, for instance, analyzing the LD-to-SMF coupling system with or without the coupling optics. Under these circumstances, the analytical expression of the far-field intensity distribution is essential.

And finally, a simple expression of the loss of the LD-to-SMF coupling system was deduced by the statistical parameter, namely, the rms value, of the near-field phase, which gives out a quantitative analysis of the loss of the LD-to-SMF coupling system induced by the deviation of the LD far-field intensity distribution from ideal elliptical Gaussian, which previously was only vaguely expressed by a factor in the range of 0.1 to 1 dB.

References

1. H. Kogelnik, "Coupling and Conversion Coefficients for Optical Modes," in J. Fox, ed., *Microwave Research Institute Symposia Series,* vol. 14, pp. 333–347. Brooklyn, NY: MRI, 1964.
2. W. Bludau and R. H. Rossberg, "Low-Loss Laser-to-Fiber Coupling with Negligible Feedback," *IEEE J. Lightwave Technol.* **LT-3**, 294–302, 1985.
3. S. Geckeler, *Optical Fiber Transmission Systems,* pp. 147–157. Norwood, MA: Artech House, 1987.
4. H. Karstensen, "Laser Diode to Single-Mode Fiber Coupling with Ball Lenses," *J. Opt. Commun.* **9**, 42–49, 1989.
5. J. M. Elson, H. E. Bennett, and J. M. Bennett, "Scattering from Optical Surfaces," in R. R. Shannon and J. C. Wyant, eds., *Applied Optics and Optical Engineering,* vol. VII, pp. 191–244. New York: Academic Press, 1979.
6. P. Herre and U. Barabas, "Fine Structure of the Far-Fields of 1.3 μm Laser Diodes," *AEÜ* **41,** 10–12, 1978.
7. M. Sumida and K. Takemoto, "Lens Coupling of Laser Diode to Single-Mode Fibers," *IEEE J. Lightwave Technol.* **LT-2**, 305–311, 1984.
8. J. Lipson, R. T. Ku, and R. E. Scott, "Opto-mechanical Considerations for Laser-Fiber Coupling and Packaging," *1985 Int. Lens Design Conf., Proc. SPIE* **554**, 308–312, 1986.
9. K. Kawano, "Coupling Characteristics of Lens System for Laser Diode Modules Using Single-Mode Fiber," *Appl. Opt.* **25**, 2500–2605, 1986.
10. T. Sugie and M. Saruwatari, "Distributed Feedback Laser Diode (DFB-LD) to Single-Mode Fiber Coupling Module with Optical Isolator for High Bit Rate Modulation," *IEEE J. Lightwave Technol.* **LT-4**, 236–245, 1986.
11. H. M. Presby, N. Amitay, R. Scotti, and A. Benner, "Simplified Laser to Fibre Coupling via Optical Fibre Up-Tappers," *Electron. Lett.* **24**, 323–324, 1988.
12. B. Hillerich, "Aberration Induced Coupling Loss of Micro-Lenses Used for LDs and LEDs to Single-Mode Fiber Coupling," *Tech. Digest Optical Fiber Communications Conf.*, New Orleans, paper THI2, 1988.